

Development and Testing of 140 GHz Absorber Coatings for the Water Baffle of W7-X Cryopumps

Miriam Floristán^{a, b}, Philipp Müller^b, Andreas Gebhardt^b, Andreas Killinger^b, Rainer Gadow^b, Antonio Cardella^c, Chuanfei Li^d, Reinhold Stadler^d, Günter Zangl^d, Matthias Hirsch^d, Heinrich P. Laqua^d, Walter Kasperek^e

^a Graduate School for advanced Manufacturing Engineering (GSaME), Universität Stuttgart

^b Institute for Manufacturing Technologies of Ceramic Components and Composites (IMTCCC), Universität Stuttgart, Allmandring 7 b, D-70569 Stuttgart, Germany

^c European Commission c/o Wendelstein 7X, Boltzmannstraße 2, D-85748 Garching, Germany

^d Max-Planck-Institut für Plasmaphysik, EURATOM Assoc., Wendelsteinstraße 1, D-17491 Greifswald, Germany

^e Institut für Plasmaforschung, Universität Stuttgart, Pfaffenwaldring 31, D-70569 Stuttgart, Germany

Due to the relatively high strayfield radiation (140 GHz) from the electron cyclotron radio frequency heating system to which the W7-X cryopumps are expected to be subjected, coating systems acting as an efficient absorber for 140 GHz radiation have been developed for the water-cooled baffle shield in order to reduce the thermal load on the liquid N shield and the liquid He cryopanel.

Several types of oxide ceramic coatings were applied on planar copper substrates by Atmospheric Plasma Spraying. The influence of the process parameters on the coating properties and microwave absorbing capability was analyzed. It was found that film thickness and microstructure of the sprayed coatings have a significant influence on microwave absorption behaviour. For Al₂O₃/TiO₂ coatings, absorption values over 90% were obtained for the 140 GHz probing beam.

After optimization of the coating structure for maximum microwave absorption, the coating procedure was adapted by special robot trajectories to the complex water baffle geometry. The selected spray parameters and kinematics were then used for the complete coating of four mock-ups, which have been tested in the W7-X strayfield test facility Mistral. The mock-ups showed absorption values of 75%.

Keywords: Wendelstein 7-X Cryopump, Atmospheric Plasma Spraying, microwave absorption, Al₂O₃/TiO₂ coatings, coating thickness.

1. Introduction

The extreme operating conditions of fusion reactor devices have lead to an increasing interest in the field of high performance materials. Research has focused on the development of new materials, which can work under thermal and mechanical loads or strong radiation.

Cryopumps in Wendelstein 7-X are subjected to high strayfield microwave radiation from the electron cyclotron radio frequency heating system. In order to protect the He cryopanel, chevrons are used. Chevrons are composed by several copper lamellas, which absorb the radiation from the plasma. However, the stray radiation level at the cryopump is not sufficiently reduced by the Cu chevrons. Therefore, microwave absorbing ceramic coatings applied on the chevrons were investigated with the aim of reducing the thermal load on the cryopanel.

Some publications have pointed out the potential of Al₂O₃/TiO₂ thermally sprayed coatings for diverse applications on components of fusion reactors [1-3]. However, scarce information is found in the literature about the optimal processing of these coatings regarding their absorption capability and about the influence of the powder and phase composition on the functionality of

the coatings. In this study Al₂O₃/TiO₂ coating systems were developed and optimized to be deposited on water baffles.

2. Materials and methods

Atmospheric Plasma Spraying is a flexible and cost effective coating process characterised by the high reached temperatures, which allow the processing of almost any material. An electric arc is created between an anode and a cathode in the spray torch. A gas mixture is injected and due to its interaction with the electric arc, a plasma jet is generated. The spray powder is melted in the plasma jet and propelled towards the substrate surface. Upon impacting at the surface, the particles deform and rapidly solidify, building up the coating.

Coating experiments were carried out on planar copper substrates (50 x 50 x 2 mm³) to determine the optimal spray parameters for the application. The F6 APS torch (GTV, Germany) was used in this study. The gun was guided by a six axis robot (Type RX 130 B, Stäubli Tec-Systems GmbH, Germany) and described a meander movement to cover the samples. The substrates were degreased using acetone and in order to enhance

the mechanical adhesion of the coating to the substrate, they were grit blasted prior to coating with 250 μm alumina grit, pressure of 0.6 MPa at an angle of 90° and distance of approximately 200 mm.

All the samples were characterised regarding their microwave absorption behaviour as described in [4]. The measurements were taken with parallel and perpendicular polarisation, and in each case with incidence angles of 20°, 45° and 60°.

The Microwave Stray Radiation Launch facility, MISTRAL, which allows the testing of in-vessel components of W7-X in an environment of isotropic 140 GHz radiation [5], was used to test the final coated mock-ups.

3. Results

3.1 Influence of the spray angle on the coating microstructure and functionality

Spray angle is the angle between the center axis of the plasma torch and the surface of the substrate, in the plane orthogonal to the torch displacement [6]. Due to the complex geometry of the water baffle, it is not possible to perform the spray operation continuously perpendicular to the chevrons surface. Instead, spray angles lower than 90° are necessary in order to reach with the plasma jet all the areas of the chevrons. Therefore, the influence of lower spray angles on the coating microstructure and absorption capability was analysed.

Planar substrates were coated with $\text{Al}_2\text{O}_3/\text{TiO}_2$ 87/13 wt.% with a constant thickness of 150 μm and varying spray angle of 90°, 70°, 50° and 30°. In Fig. 1, micrograph cross sections of the coatings, as well as SEM pictures of the layer surfaces are shown.

With a reduction of the spray angle, the tangential component of the velocity of the in-flight particles during spraying is enhanced. This strongly influences the deformation of the particles into splats at impact with the substrate. Low spray angles lead to the formation of more elongated splats orientated in the direction of spraying [6], as can be seen in Fig. 1. Moreover, saw tooth profiles arise with low spray angles [7], as it was observed for the sample sprayed with 30°. As a consequence, impinging particles cannot cover some regions that are shadowed in the saw tooth, leading to the formation of pores. Increased coating roughness and low deposition efficiency are also characteristic of off-normal spray angles [6].

Microwave absorption measurements were performed on the samples. As can be seen in Fig. 2, the absorption of the coatings is comparable for samples sprayed with angles between 90° and 50°, and it drops strongly for the spray angle 30°. This behaviour is related to the highly inhomogeneous coating microstructure characterized by high porosity and roughness obtained with low spray angles.

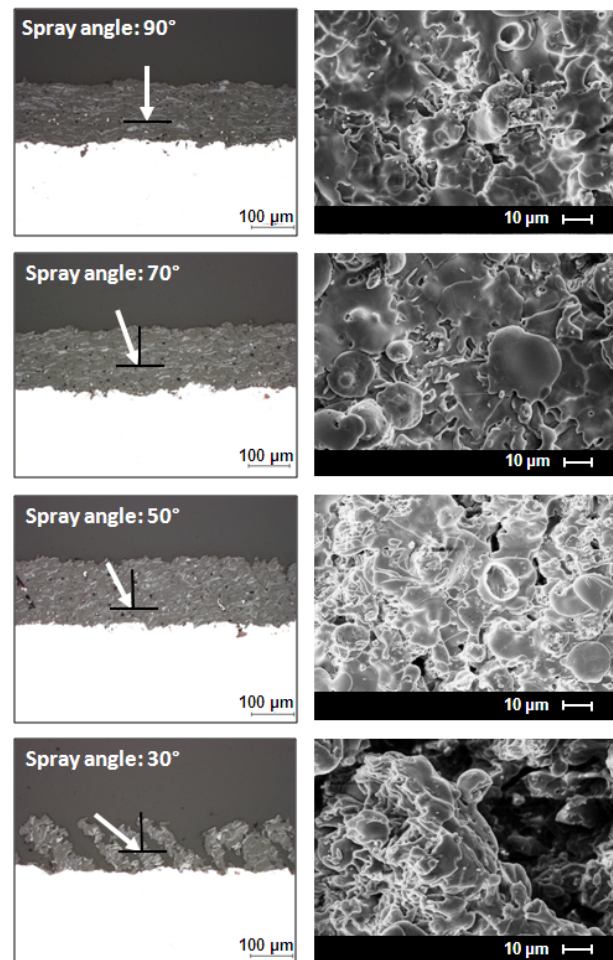


Fig. 1: Cross section micrographs and SEM pictures of the coatings surfaces deposited with spray angles between 90° and 30°.

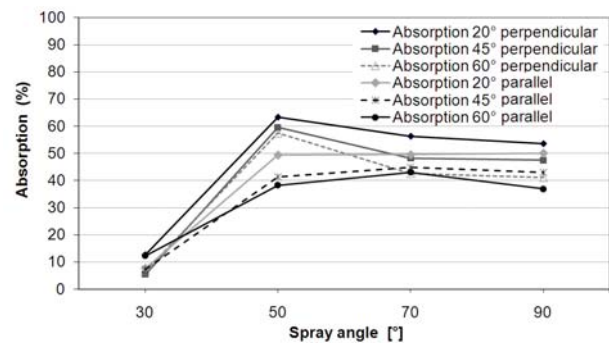


Fig. 2: Coating microwave absorption depending on the spray angle.

3.2 Material screening

Al_2O_3 and TiO_2 powders, as well as their mixtures in different compositions and crystalline phases, were sprayed on Cu plates with a fixed thickness of 150 μm . Two additional ceramics were tested; Cr_2O_3 and ZrO_2 , see Fig. 3. All the powders had particle size distributions of $-20+5 \mu\text{m}$. The pure oxide ceramic materials analysed showed low absorption values. The best absorption was found with $\text{Al}_2\text{O}_3/\text{TiO}_2$ mixed powders, improving the absorption capability by increasing the content of TiO_2 .

Further analysis of the mixed ceramic coatings was carried out. $\text{Al}_2\text{O}_3/\text{TiO}_2$ spray materials with composition 87/13 and 50/50 were selected for investigation. For each mixed powder composition, two different powders in particle size were used: $-20+5 \mu\text{m}$ and $-40+10 \mu\text{m}$. All the used spray powders are commercially available and produced by fusion methods.

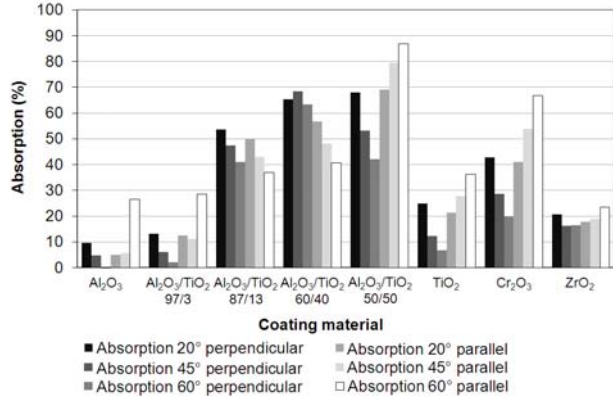


Fig. 3: Coating microwave absorption for different sprayed materials.

Several samples were sprayed with each powder obtaining coatings with varying thickness from $50 \mu\text{m}$ to $250 \mu\text{m}$. It was found that the microwave absorption of the layers is strongly determined by its thickness, and that for each powder the thickness range for an optimal absorption differs. The results are shown in Fig. 4, in which for each spray material, an averaged absorption value for all measurements at different angles of incidence and polarisations is displayed.

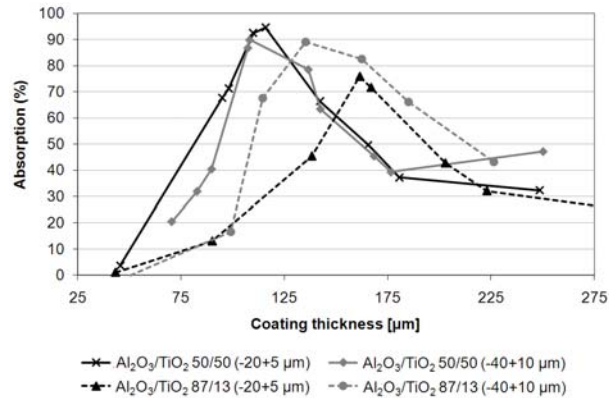


Fig. 4: Coating microwave absorption as a function of the coating thickness.

In the case of the $\text{Al}_2\text{O}_3/\text{TiO}_2$ 87/13 spray powder, the coarse material presents a wider area with optimal absorption for 140 GHz radiation in comparison with the finer powder. This effect is less clearly visible for the 50/50 composition.

3.3 Coating characterisation

The best absorbing coatings of each of the four powders analysed were characterised, see Table 1, obtaining typical values of plasma sprayed coatings, which are suitable for the application of study. For each coating system, the microstructure and analysed properties were comparable for samples with a thickness of $\pm 50 \mu\text{m}$ in comparison with the optimum layer thickness. This is important regarding the coating of the real components, in which due to the complex component geometry, the coating thickness cannot be kept constant over the whole surface.

The state of residual stresses in thermally sprayed composites, which arise as a result of temperature gradients, differences in thermophysical material properties and the cooling and solidification process, affect the structural properties of the coating, as well as its functionality and reliability [8]. Residual stress measurements were carried out using the micro-hole milling and drilling method [8], see Fig. 5.

The four coating systems show very low stresses. At the coating surface all the layers present tensile stresses, except the $\text{Al}_2\text{O}_3/\text{TiO}_2$ 50/50 with powder size distribution $-20+5 \mu\text{m}$. The high thermal conductivity characteristic of Cu may greatly reduce the cooling stresses, which are in this case of compressive nature due to the higher CTE of Cu in comparison to the $\text{Al}_2\text{O}_3/\text{TiO}_2$ coating. The 50/50 coatings present higher content of Al_2TiO_5 , which has a CTE ($25-1100^\circ\text{C}$) of $0.05-1.6 \text{ 1/K } 10^{-6}$ [9]. Therefore, the difference in CTE between substrate and coating may be stronger than for the 87/13, and consequently the residual stresses tend to compression.

In some publications, the use of bond coatings to reduce residual stresses was analysed for microwave absorbing coatings on Cu substrates [1]. In this study, the residual stresses in the composite system were low and the use of a bond coating was not necessary.

Table 1: Characterisation of the coatings with best microwave absorption for each $\text{Al}_2\text{O}_3/\text{TiO}_2$ powder.

Coating system	Coating thickness [μm]	Average microwave absorption (%)	Coating porosity (%)	Coating roughness Rz [μm]	Micro-hardness HV 0.1	Coating adhesion [MPa]	Phase composition
$\text{Al}_2\text{O}_3/\text{TiO}_2$ 87/13, $-20+5 \mu\text{m}$	161.54	75.85	2.06	29.87	976.43	9.97	$\alpha\text{-Al}_2\text{O}_3$, $\gamma\text{-Al}_2\text{O}_3$ Rutile
$\text{Al}_2\text{O}_3/\text{TiO}_2$ 87/13, $-40+10 \mu\text{m}$	135.29	89.18	4.2	36.24	977.41	14.53	$\alpha\text{-Al}_2\text{O}_3$, $\gamma\text{-Al}_2\text{O}_3$ Rutile
$\text{Al}_2\text{O}_3/\text{TiO}_2$ 50/50, $-20+5 \mu\text{m}$	115.94	94.68	2.32	27.68	919.35	18.95	$\gamma\text{-Al}_2\text{O}_3$ Rutile, Al_2TiO_5
$\text{Al}_2\text{O}_3/\text{TiO}_2$ 50/50, $-40+10 \mu\text{m}$	108.33	89.91	2.04	31.78	846.46	25.41	$\gamma\text{-Al}_2\text{O}_3$ Rutile, Al_2TiO_5

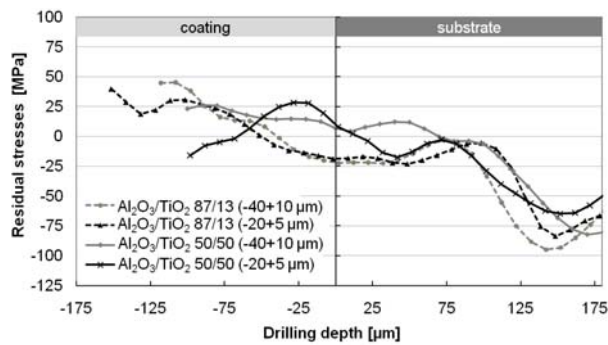


Fig. 5: Residual stress measurements of the best absorbing coatings of each analysed $\text{Al}_2\text{O}_3/\text{TiO}_2$ coating system.

Samples were subjected to outgasing and thermocycling tests. No delamination or mechanical damage of the coatings was detected. Infrared measurements were carried out on the samples. All the coatings presented emission coefficients over 0.9.

The powders $\text{Al}_2\text{O}_3/\text{TiO}_2$ 50/50 and 87/13, both with grain size distribution of $-40+10 \mu\text{m}$, were selected as the ones with best performance and highest potential for the application of study and were used for the coating of the mock-up prototypes.

3.4 Kinematic optimization

The coating process optimised for plane substrates had to be adapted to the real and complex geometry of the water baffle. With this aim, the robot kinematics, which describe the movement of the spray torch, were adapted to the component geometry.

However, as seen in section 3.1, changes in the spray angle produce modifications in the coating build-up and microstructure. Therefore, several optimisation iterations were needed to determine the number of coating cycles, meander offset and combination of spray angles needed to cover the highest surface of the component, keeping constant coating thickness at the corresponding values to achieve high absorption rates, and obtaining adequate adhesion and coating mechanical stability. In Fig. 6, an image of the coated mock-up is shown.



Fig. 6: Coated mock-up.

3.5 Mistral test

Four mock-ups were coated for Mistral-test; two of them with the optimised system of $\text{Al}_2\text{O}_3/\text{TiO}_2$ 50/50 and two with 87/13, all with powder grain size distribution of $-40+10 \mu\text{m}$. An uncoated mock-up was as well tested.

The Mistral chamber was operated with a power of 5 kW. Quantitative measurements were made by calorimetry obtaining the total absorbed load P_{total} . From this load, 0.64 kW were absorbed by the cooling system (stainless steel tubes and pipes), and the rest by the mock-up. For an isotropic power flux density of 30 kW/m^2 , and considering that the effective surface of the chevrons lamellas is 891 cm^2 , a chevron with absorption coefficient of 100% absorbs 2.67 kW. In table 2, the results of the tests are shown. The measurements made indicate that the coatings extract over to 2 kW of the 5 kW input power.

Table 2: Results of the Mistral test.

Sample	P_{total} [kW]	P_{mockup} [kW]	Absorption (%)
Uncoated mock-up	0.77	0.13	4.8
Mock-up $\text{Al}_2\text{O}_3/\text{TiO}_2$ 87/13	2.66	2.02	75.7
Mock-up $\text{Al}_2\text{O}_3/\text{TiO}_2$ 50/50	2.25	1.61	60.3

4. Summary

Plasma sprayed $\text{Al}_2\text{O}_3/\text{TiO}_2$ with different composition and powder grain size distribution were tested regarding their microwave absorption capability at a frequency of 140 GHz. It was found that coating thickness, grain size and composition (Al_2O_3 - TiO_2 ratio) strongly influence the system absorption. Coated mock-ups tested in Mistral showed absorption up to 75.7% in the case of $\text{Al}_2\text{O}_3/\text{TiO}_2$ 87/13 coatings.

References

- [1] N. Spinicchia, G. Angella, R. Benocci, A. Bruschi, A. Cremona, G. Gittini, A. Nardone, E. Signorelli, E. Vassallo, Surf. Coat. Technol. 200 (2005) 1151-1154.
- [2] A. Bruschi, S. Cirant, F. Gandini, G. Granucci, V. Mellera, V. Muzzini, A. Nardone, A. Simonetto, C. Sozzi, N. Spinicchia, Nucl. Fusion 43 (2003) 1513-1519.
- [3] F. Brossa, G. Rigon, B. Looman, Jour. Nucl. Mater. 155-157 (1988) 267-272.
- [4] R. Wacker, F. Leuterer, D. Wagner, H. Hailer, W. Kasperek, in: Proceedings of the 27th International Conference on Infrared and millimeter Waves, IEEE Press, New York, 2002, pp. 159-160.
- [5] Ullrich S., Charakterisierung einer materialtestkammer als millimeterwellen-resonator bei 140 GHz, Diploma Thesis University of Greifswald, 2005 (summary in Stellarator News 98 (May 2005)) available on the web: <http://www.ornl.gov/sci/fed/stelnews/>.
- [6] G. Montavon, S. Sampath, C.C. Berndt, Herman H., C. Coddet, Surf. Coat. Technol. 91 (1997) 107.
- [7] M. F. Smith, R.A. Neiser, R.C. Dykhuizen, in: Proceeding of the 7th National Thermal Spray Conference, C.C. Berndt., ASM International, Materials Park, Ohio, 1995, pp. 603.
- [8] M. Wenzelburger, D. López, R. Gadow, Surf. Coat. Technol. 201 (2006) 1995-2001.
- [9] I.J. Kim, K. S. Lee, C. G. Aneziris, Key Eng. Mat. 336-338 (2007) 2448-2450.